



Component-Method Analysis of Composite Beam-to-Column Joints with a Non-Extended End Plate

Rachid Slimani¹, Mehdi Seghiri^{2*}, Abderrahmane Menasria³, Kadidja Sekhri⁴

¹University of Tamanghasset, Faculty of Sciences & Technology, Sciences & Technology Department, BP 10034, Sersouf Tamanghasset city 11000, Algeria

Email slimanirachid43@yahoo.fr - ORCID: 0000-0002-205232-9863

²University of Tamanghasset, Faculty of Sciences & Technology, Sciences & Technology Department, BP 10034, Sersouf Tamanghasset city 11000, Algeria

* Corresponding Author Email: seghirimehdi25@gmail.com - ORCID: 0000-0001-5332-4840

³Materials and Hydrology Laboratory, University of Sidi Bel Abbes, University of Khenchela, Faculty of Sciences and Technology, Civil Engineering Department, BP 1252 Road of Batna Khenchela, Khenchela city 40000, Algeria

Email: hbb2483@gmail.com - ORCID: 0009-0008-3507-0128

⁴LGC-ROI, civil engineering laboratory-risks and structures in interactions, department of civil engineering, Faculty of Technology, university of Batan2, batna city 05001, Algeria,

Email: K.sekhri@univ-batna2.dz - ORCID: 0009-0009-3166-847X

Article Info:

DOI: 10.22399/ijcesen.5117

Received : 29 November 2025

Revised : 15 April 2026

Accepted : 20 April 2026

Keywords

Mechanical characteristics
non-extended end plate
composite joints

Abstract:

Composite beam-to-column joints significantly influence the global stiffness, strength, and force redistribution capacity of steel-concrete composite frames. Although the Eurocode component method provides a rational basis for characterization joint, its manual application remains time-consuming and error-prone, which limits its systematic use in design and parametric assessment. This study applies the Eurocode 3/Eurocode 4 component method to composite beam-column joints with a non-extended end plate, and develops a dedicated calculation program to evaluate the joint design moment resistance ($M_{j,Rd}$) and initial rotational stiffness ($S_{j,ini}$) and to support parametric studies. The parametric results show that increasing the slab longitudinal reinforcement ratio can raise ($M_{j,Rd}$) by up to 27.53% (limited end-plate configuration) and increase ($S_{j,ini}$) by up to 122.416% (non-extended end plate configuration). Increasing the beam section height enhances ($M_{j,Rd}$) by up to 83.068%, while the stiffness advantage of the flush end plate over the limited end plate can reach 110.944%. The end-plate thickness exhibits a saturation effect: beyond a threshold thickness close to flange thickness of profile t_{fc} , further increases provide negligible gains in ($M_{j,Rd}$) and ($S_{j,ini}$). These findings provide practical guidance for optimizing joint detailing and avoiding unnecessary over-dimensioning, while the developed software enables rapid Eurocode-consistent evaluation of composite joint performance.

1. Introduction

Steel-concrete composite construction is widely used in buildings and civil engineering structures because it combines the tensile strength and ductility of steel with the compressive resistance, stiffness, durability, and fire protection provided by concrete [1], [2]. The basic mechanical rationale of composite construction is that concrete is mobilized primarily in compression while steel resists tension and provides ductility. This complementary action

improves member stiffness, limits local instability of slender steel elements, and supports efficient long-span structural solutions. A schematic distinction between non-composite and composite beam behavior is shown in Figure 1. Within such systems, beam-to-column joints are critical structural zones because they control force transfer, rotational restraint, stiffness distribution, redistribution capacity, and the development of local or global failure mechanisms. Their role is therefore central not only in gravity-load-resistant frames, where

stiffness and serviceability are important, but also in seismic-resistant frames, where joint ductility, degradation, and energy dissipation

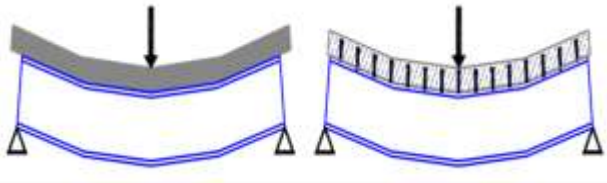


Figure 1. (a): Non-mixed beam, (b): mixed beam

strongly influence the global behavior of the frame[3], [4], [5], [6], [7], [8], [9], [10], [11], [12], [13], [14], [15], [16]. In practice, composite joints seldom behave as perfectly pinned or perfectly rigid. Rather, their response is usually semi-rigid, and this intermediate behavior may significantly modify internal-force distribution, drift demand, and the localization of inelastic deformations. Among practical beam-to-column connection typologies, end-plate bolted joints remain particularly common because of their fabrication simplicity, ease of erection, bolted assembly, and adaptability to different structural demands [17], [18]. In steel–concrete composite joints subjected to hogging bending moment, the slab longitudinal reinforcement becomes an active tensile component and may significantly contribute to both joint resistance and initial rotational stiffness. Experimental and numerical studies have shown that slab participation may alter the moment–rotation response, increase stiffness and resistance, and modify the governing failure mode when compared with the corresponding bare steel connection [19], [20]. This is especially relevant for flush or non-extended end-plate composite joints, where the contribution of the slab, the distribution of bolt-row forces, and the flexibility of the end plate and panel zone interact closely. In the present work, particular attention is given to the non-extended end-plate

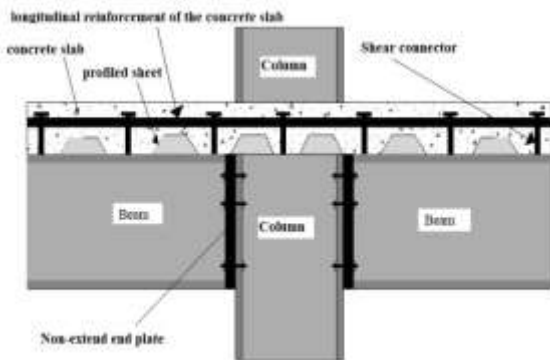


Figure 2. Beam-to-column composite joints with end plate.

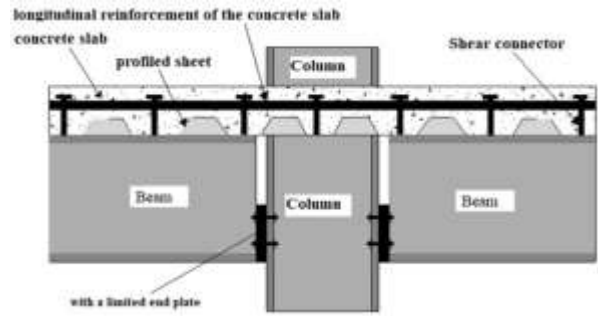


Figure 3. Beam-to-column composite joints with limited end plate.

composite joint shown in Figure 2, with comparative reference to the limited end-plate configuration shown in Figure 3. Historically, joint characterization has relied on three main approaches: experimental testing, finite element modelling, and analytical/component-based modelling. Experimental studies remain indispensable because they reveal actual failure mechanisms, crack development, local deformation modes, bond-slip effects, and cyclic degradation phenomena that are difficult to idealize a priori [19], [5], [20]. However, testing is expensive and limited in parametric coverage. Finite element modelling can capture local contact effects, cracking, yielding, prying action, and instability in much greater detail and has been used successfully for both steel and composite joints[21], [22], [23], [16]. Yet, high-fidelity numerical models require significant calibration effort, computational resources, and specialist expertise, which limits their use for routine design and broad parametric studies.

For this reason, the component method has become the principal analytical framework for design-oriented characterization of joints. It is the approach recommended by the Eurocodes for both steel and composite joints and is based on decomposing a joint into a set of individual mechanical components, assigning each component its own stiffness and resistance, and assembling these contributions to predict the global joint response [1], [2]. [24] emphasized that this is the reference Eurocode-based procedure for joint characterization, while [25] further highlighted that it remains one of the most appropriate analytical tools for extending joint design beyond the loading situations explicitly covered in current provisions. In composite joints, Eurocode 4 supplements the steel-joint framework with additional components related to slab reinforcement in tension and concrete-related compression mechanisms.

Despite its strengths, the current codified application of the component method remains incomplete for several practically relevant composite-joint situations. Existing Eurocode provisions mainly cover composite joints under shear forces and hogging moments, while real joints may also be subjected to sagging moments, cyclic loading, combined bending and axial force, elevated temperatures, and exceptional loading conditions such as column removal [24], [25], [26]. This limitation has motivated a series of studies aimed at extending analytical characterization beyond current Eurocode provisions. [27], for example, showed that the application of the component method to composite joints under sagging moment requires explicit characterization of the missing component (concrete slab in compression.) These studies confirm that the component method is conceptually robust, but that its practical implementation still depends on the availability of reliable component models for the joint configuration and loading case under consideration.

Recent literature has also broadened the understanding of the role of key parameters in composite beam-to-column connection behavior. [28] showed that stiffness and resistance are strongly affected by reinforcement ratio, slab type, steel-concrete interaction, moment direction, and geometric section properties. [16] reported that end-plate thickness, section proportions, and local detailing significantly influence stiffness, moment resistance, and failure mode. [20], in a full-scale experimental study of exterior composite joints with flush end plate and precast slab, showed that the degree of shear connection and the effective longitudinal reinforcement ratio significantly affect stiffness, flexural capacity, and ductility. [29] similarly demonstrated under cyclic loading that the behavior of external composite joints is sensitive to reinforcement size, connector diameter, and end-plate detailing, while realistic joint classification remains essential under Eurocode concepts.

Despite substantial advancements in the literature, some gaps persist that are directly pertinent to the current investigation. Although most studies address steel end-plate joints or other composite joint typologies, composite beam-to-column joints with a non-extended end plate remain less systematically treated within a unified eurocode [1], [2] component-method framework. Additionally, even when the component method is available, its manual implementation becomes cumbersome and error-prone when several interacting components and multiple design variables must be evaluated simultaneously. Among the practical geometric variables influencing composite joint behavior,

beam section height deserves particular attention because it modifies the internal lever arm, connection stiffness, and relative contribution of the end plate, yet it remains less explicitly foregrounded than slab reinforcement and end-plate detailing in many analytical studies. Furthermore, the influence of practical variables such as slab longitudinal reinforcement ratio, beam section height, end-plate thickness, column encasement, and bolt-row arrangement has not been sufficiently synthesized for this specific joint type within a practical analytical environment.

The present study applies the Eurocode [1], [2] component method to composite beam-to-column joints with a non-extended end plate and develops a dedicated calculation program for evaluating two key design-oriented mechanical characteristics of the joint: the design moment resistance $M_{j,Rd}$ and the initial rotational stiffness $S_{j,ini}$. and a systematic parametric investigation of the effect of slab longitudinal reinforcement ratio, beam section height, end-plate thickness, column encasement condition, and the presence of a second row of tension bolts on the global joint response.

Accordingly, the objective of the paper is to quantify how these parameters influence $M_{j,Rd}$ and $S_{j,ini}$, and to compare the behavior of composite joints with non-extended and limited end plates in order to provide practical guidance for connection optimization and for avoiding unnecessary over-dimensioning in design. The novelty of the work lies not in proposing a new mechanical model, but in translating the codified component-method procedure into a dedicated computational software that makes the evaluation of ($M_{j,Rd}$) and ($S_{j,ini}$) rapid, systematic, and suitable for extended parametric analysis of this joint configuration.

1.1 Composite beam-to-column joints and their significance

Steel-concrete composite joints are key structural zones because they govern force transfer, rotational restraint, stiffness, resistance, and redistribution capacity. Their importance is amplified in both gravity-load-resistant and seismic frames, since the local behavior of the joint affects the global response of the structure, including drift, stability, and inelastic mechanism formation [3], [5], [6]. Unlike idealized pinned or rigid joints, actual composite beam-to-column joints generally behave as semi-rigid systems, and their response depends on the interaction among steel members, bolts, end plates, slab reinforcement, shear connection, and concrete-related compression zones ([2], [1]). Recent studies confirm that composite action can substantially

enhance joint stiffness and strength, but the improvement is not uniform and depends strongly on connection detailing. [28] showed that composite beam-to-column connections are highly sensitive to reinforcement ratio, slab type, steel–concrete interaction, moment direction, and section geometry. [20] found that, in exterior composite joints with flush end plate and precast slab, both the degree of shear connection and the effective longitudinal reinforcement ratio significantly affected stiffness and flexural capacity. [29] reported comparable findings under cyclic loading, where central reinforcement bars, bolted shear connectors, and end-plate detailing all influenced moment capacity, stiffness, and ductility.

1.2 End-plate joints and local detailing effects

End-plate joints remain particularly common because they are easy to fabricate and erect, adaptable to bolted assembly, and capable of providing different levels of stiffness and strength [17], [18]. However, their behavior is strongly dependent on local parameters such as end-plate thickness, bolt diameter and arrangement, beam and column dimensions, stiffeners, contact conditions, and pretension forces [22], [23], [30].

[22] showed through validated nonlinear finite element analyses that end-plate thickness and stiffener arrangement significantly affect joint stiffness, strength, force redistribution, and failure mode. [23] similarly demonstrated that local stiffening can modify the initial rotational stiffness and even change the Eurocode-based classification of a joint. [31] found that flush and extended end-plate joints respond differently under combined bending and axial force, with flush end-plate joints being more sensitive to axial load effects. These findings indicate that even within steel joints, end-plate geometry and detailing substantially alter behavior; for composite joints, where slab participation adds further complexity, this sensitivity is expected to be even more pronounced.

1.3 Component method as the theoretical framework

The component method is the most established analytical framework for design-oriented joint characterization. [24] described it as the Eurocode-based reference procedure for predicting the mechanical properties of joints, including stiffness, resistance, and ductility. [25] further emphasized that the component method remains the most appropriate analytical basis for extending design rules beyond currently codified loading situations.

The method idealizes the joint as an assembly of individual components, each represented by mechanical springs with their own strength and stiffness properties. Its application requires three essential steps: identifying the active components, characterizing the mechanical properties of each component, and assembling them to obtain the global joint response [24], [25].

For composite joints, the component method extends the steel-joint framework by including composite-specific components, notably the longitudinal reinforcement in tension and compression-related slab/concrete components recognized in Eurocode 4 [1]. This makes it particularly suitable for composite beam-to-column joints in hogging regions, where slab reinforcement participates directly in the tension zone.

1.4 Limitations of current Eurocode provisions

A major limitation in the current state of the art is that Eurocode provisions for composite joints remain incomplete for several practically relevant loading cases. [25] explicitly noted that the current rules mainly cover composite joints subjected to shear forces and hogging moments, but not adequately sagging moments, cyclic loading, combined bending and axial load, or elevated temperatures. [25] reinforced this broader view and highlighted the need to move (from Eurocodes and beyond) when dealing with real design situations involving seismic actions, fire, robustness, or exceptional events.

This issue is illustrated by [32], who studied composite joints under sagging moment and identified the concrete slab in compression as the missing component needed to apply the component method in that case. Through finite element simulations and analytical development, they proposed a model for the effective slab width and the slab-in-compression component, showing that analytical extension of the component method is both possible and necessary when code provisions are incomplete.

1.5 Experimental, numerical, and analytical approaches

No single approach is sufficient on its own to fully characterize composite joints. Experimental studies remain indispensable for identifying actual failure mechanisms, crack development, slip, panel deformations, and interaction effects [19], [5], [33], [34], [35], [36], [20]. Finite element analyses provide greater access to local stress redistribution, contact behavior, cracking, prying action, bolt-force

evolution, and local instability ([30], [22], [37], [38], [39], [40], [16]). Analytical approaches, especially the component method, remain essential for practical design because they provide a rational and efficient means to estimate joint stiffness and resistance. The literature therefore supports a complementary view: experiments reveal the mechanisms, FE models clarify them in detail, and analytical models translate them into design procedures.

1.6 Joint classification under Eurocode

Eurocode classification of joints as rigid, semi-rigid, or pinned is central because it determines how the joint should be represented in global structural analysis. [2], [1] provide the conceptual basis for this classification. Recent studies confirm that many practical composite beam-to-column joints fall within the semi-rigid range. [28] reported that most of the analyzed composite double web-angle joints were semi-rigid, although some could be classified as rigid depending on the parameter combination. [20] and [29] likewise showed that composite joint behavior should be described through moment-rotation response and not by idealized rigid-pinned assumptions alone.

1.7 Most parametric effects on composite joint behavior

Recent studies consistently show that slab reinforcement is important, although the relationship may not always be strictly monotonic. [20] reported that increasing the effective longitudinal reinforcement ratio improved stiffness, load capacity, and ductility in exterior composite joints with flush end plate. [28] found that a negative reinforcement ratio of 0.75% yielded the highest stiffness in the studied connection family. [27] also showed that insufficient reinforcement may trigger premature failure in slab-related joint mechanisms. Geometric parameters also emerge repeatedly as major predictors of joint response. [28] showed through feature-importance analysis that section geometry was among the most influential variables governing connection stiffness and resistance. [16] demonstrated that section proportions and local composite-column geometry strongly affect end-plate joint performance. [26] further showed that slab-related geometric features such as profiled sheeting direction can markedly affect the resistance and rotation of composite joints under exceptional loading. Despite this, the specific effect of beam section height has not been sufficiently foregrounded in Eurocode-based analytical studies of non-extended composite end-plate joints.

End-plate thickness is also consistently reported as a key parameter. [22] showed that it has a major influence on initial stiffness, ultimate strength, and failure mode in steel end-plate joints. [16] also reported that reducing end-plate thickness in composite end-plate joints led to earlier plastic deformation and cracking. The role of bolt rows and shear connection is similarly important, since force redistribution and slip behavior are highly sensitive to connection detailing ([22], [29], [20]).

The reviewed literature establishes that composite beam-to-column joints exhibit semi-rigid behavior that depends strongly on slab participation, member geometry, and local connection detailing. It also shows that the component method remains the most rational analytical basis for design-oriented characterization, but that current Eurocode provisions do not fully cover all practical loading and configuration cases. In addition, recent experimental and numerical studies confirm the importance of parameters such as reinforcement ratio, slab type, end-plate thickness, and geometric proportions, but these effects have not yet been sufficiently synthesized for composite beam-to-column joints with a non-extended end plate within a practical Eurocode-consistent analytical tool.

Accordingly, the present study is positioned at the intersection of three needs identified in the literature: the need for Eurocode-consistent analytical characterization of practical composite joint configurations, the need for efficient tools that overcome the complexity of manual component-method calculations, and the need for a more systematic understanding of the influence of key design variables. On this basis, the present study focuses on the parameters most consistently identified in the literature as design-sensitive for composite joints, namely slab reinforcement, member geometry, and connection detailing, with particular emphasis on the effects of longitudinal slab reinforcement ratio, beam section height, end-plate thickness, and bolt-row arrangement in non-extended end-plate composite joints.

2. Material and Methods

2.1 Joint configurations and geometric parameters

The present study investigates two configurations of composite beam-to-column joints under hogging bending moment:

- Composite joints with a non-extended end plate, in which the end plate does not extend beyond the beam flanges, and the tension zone

is resisted by both the slab longitudinal reinforcement and the upper bolt rows;

- Composite joints with a limited end plate, used as a reference configuration for comparison purposes.

Both configurations feature:

- A steel I-section beam (IPE series) connected to a steel H-section column (HEB/HEA series) through a bolted end plate.
- A concrete slab with profiled steel sheeting, connected to the beam via shear connectors, providing composite action.
- Longitudinal reinforcement bars within the slab, acting in tension under hogging bending moment.
- High-strength bolts connecting the end plate to the column flange.

A total of ten composite joint assemblies (designated AMX10 to AMX17) were studied, as listed in Table 1.

Table 1. Geometric and configurational parameters used in the parametric study

Assembly ID	Column section	Beam section
AMX10	HEB 140	IPE 160
AMX11	HEB 140	IPE 180
AMX12	HEB 140	IPE 200
AMX13	HEB 140	IPE 240
AMX14	HEB 140	IPE 300
AMX15	HEB 140	IPE 330
AMX16	HEB 140	IPE 360
AMX17	HEB 140	IPE 400

For the parametric study of end-plate thickness influence, t_p was varied from 8 mm to 30 mm while all other parameters were kept constant table 2 preset the end-plate properties. The connection utilizes High-Resistance (HR) M16 bolts, Class 8.8. For the concrete slab, the adopted properties were listed in the table 4

Table 2. End-plate properties

f_{yp} (N/mm ²)	P (mm)	a_w (mm)	a_f (mm)	t_p (mm)	e_p (mm)
235	50	3	5	15	30

Table 3. Bolt properties — Grade 8.8 HR M16

f_{ub} (N/mm ²)	A_{sb} (mm ²)	H_h (mm)	H_n (mm)	d_w (mm)
800	157	13	10	26,75

Table 4. Concrete slab properties

μ	f_{ck}	f_{sk}	$E_{cm,c}$	E_s	K_{sc}	e_s
(%)	(N/mm ²)			(N/mm)	(mm)	
variable	20	40 0	29 x 10 ³	21 x 10 ⁴	10 ⁵	100

2.2 Assumptions of the analytical model

The analysis is restricted to the elastic–plastic characterization provided by the Eurocode component method. The following assumptions were adopted:

- the joint behaviour is represented by the assembly of discrete components with codified stiffness and resistance expressions;
- the design moment resistance is determined from component equilibrium using the resistance of the governing component;
- the initial rotational stiffness is obtained from the elastic stiffness of the active components represented by equivalent springs;
- the analysis is limited to monotonic loading under negative bending;
- the study focuses on the initial stiffness and design resistance of the joint.

These assumptions are consistent with the analytical scope of Eurocode [1], [2] joint characterization and define the limits of applicability of the present results.

In this context, the study is restricted to the evaluation of two design-oriented joint properties, namely the design moment resistance ($M_{j,Rd}$) and the initial rotational stiffness ($S_{j,ini}$). Full nonlinear moment–rotation curves, post-yield rotational capacity, cyclic degradation, and hysteretic behavior are outside the scope of the present work and were not investigated.

2.3 Calculation of design moment resistance

For simplified calculation, the plastic approach can be used to determine the design resistant moment. This moment is then taken as the maximum moment evaluated while satisfying the following criteria:

- Internal forces are in equilibrium with the external forces applied to the assembly.
- The design strength of no component is exceeded.
- Displacement compatibility is not considered.

In this type of assembly:

- The tension induced by bending is taken by both the reinforcement and the upper part of the steel attachment.
- The compression effort is concentrated at the level of the center of the lower footing of the beam.

For the non-extended end-plate configuration, the active components considered include: shear in the column web panel, compression in the column web, tension in the column web, bending of the column

flange, bending of the end plate, compression in the beam flange, tension in the beam web region, bolts in tension, and the longitudinal reinforcement of the slab in tension. For the limited end-plate configuration, the active components are fewer because the connection mechanism is simplified. The corresponding component arrangements are shown in Figures 4 and 5.

These figures provide the mechanical interpretation of the analytical model by identifying the components that govern the transfer of tension, compression, and shear within the joint. They therefore form the basis for the subsequent resistance and stiffness calculations.

The design moment resistance was finally calculated as $M_{j,Rd} = F_{Rd,i} \times Z$ (1)

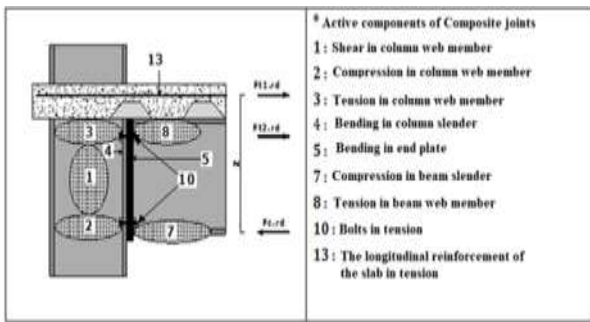


Figure 4. Components of Composite joints with a non-extended end plate.

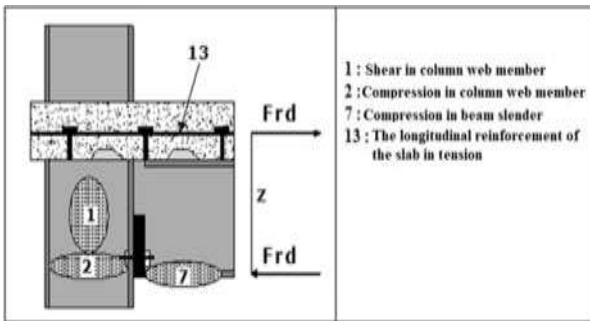


Figure 5. Components of Composite joints with limited end plate.

2.4 Initial Stiffness

It is assumed that the bolt row deformations for all rows are proportional to the distance to the compression point. The elastic force applied in each row depends on the stiffness of the components. Figure (6-b) shows how the deformations of components 3,4,5 and 10 are added to an effective spring per row of bolts, with a stiffness coefficient $K_{eff,r}$ (r: represents the row number index). Figure (6-c) shows how these effective springs per row of bolts are replaced by an equivalent spring acting at a lever arm “Z”. The stiffness coefficient of this

effective spring K_{eq} can be directly applied in the formula of $(S_{j,ini})$

$$K_{eff,r} = \frac{1}{\sum_i \frac{1}{K_{ir}}} \quad (2)$$

$$Z = \frac{\sum_r K_{eff,r} h_r^2}{\sum_r K_{eff,r} h_r} \quad (3)$$

$$K_{eq} = \frac{\sum_r h_{eff,r} h_r}{Z} \quad (4)$$

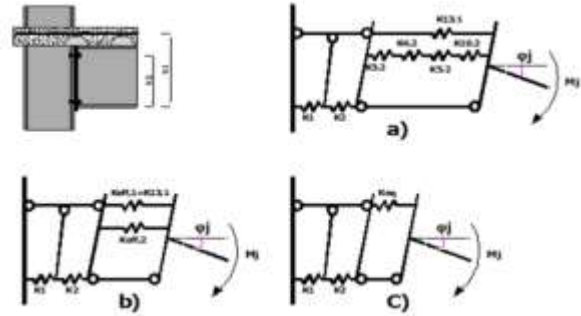


Figure 6. Spring model for a beam-column joint with a non-extended end plate.

Because the Eurocode component method requires the sequential evaluation and assembly of several interacting components, manual calculation becomes almost impossible and highly susceptible to omission and arithmetic error, especially when repeated over a wide range of geometric and material parameters. For this reason, a dedicated computational tool, denoted RIMAX-1, was developed to automate the calculation of the two key joint properties considered in this study: the design moment resistance ($M_{j,Rd}$) and the initial rotational stiffness ($S_{j,ini}$). The software was written in Delphi using object-oriented programming in Object Pascal and implements the codified formulations of Eurocode [1], [2] for the investigated joint configurations. Its main purpose is to transform a practically difficult manual procedure into a rapid and reliable design-support tool that can also be used efficiently for systematic parametric studies.

The flowcharts shown in Figures 7.a and 7.b describe the calculation logic implemented in the RIMAX-1 program for the two joint typologies. They indicate the sequence of operations starting from the reading of geometric and material input data, followed by preliminary geometric calculations, evaluation of component resistances and stiffnesses, determination of the governing joint resultant, calculation of the internal lever arm, and finally computation of the design moment resistance and the initial rotational stiffness. Thus, the flowcharts provide not only a visual summary of the

algorithmic structure, but also a direct explanation of the input–output workflow of the developed computational software.

It should be emphasized that the present work does not propose a new mechanical formulation and does not include an independent experimental validation campaign. The analytical basis of the developed program is the Eurocode [1], [2] component method, whose component resistances and stiffness expressions were originally established and calibrated through the experimental and analytical studies underlying the code provisions.

The contribution of the present study is therefore the computational implementation of this codified procedure in a dedicated Delphi environment using object-oriented programming (Object Pascal), in order to automate a calculation process that is extremely laborious and error-prone when performed manually.

B. Composite beam-to-column joints with limited end plate

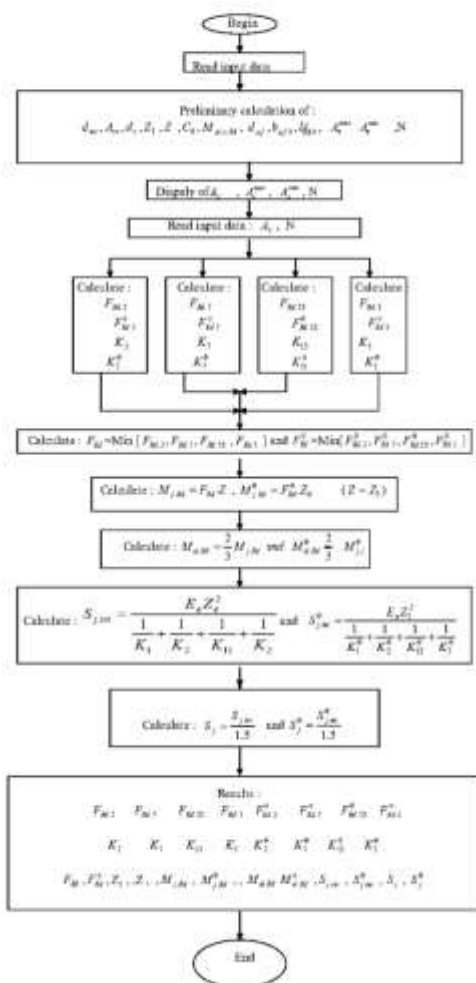


Figure 7. B- Flowchart of the RIMAX-1 computational algorithm for calculating the design moment resistance and initial rotational stiffness of composite beam-to-column joints with limited end plate based on the eurocode3/eurocode4 component method.

A. Composite beam-to-column joints with a non extended end plate

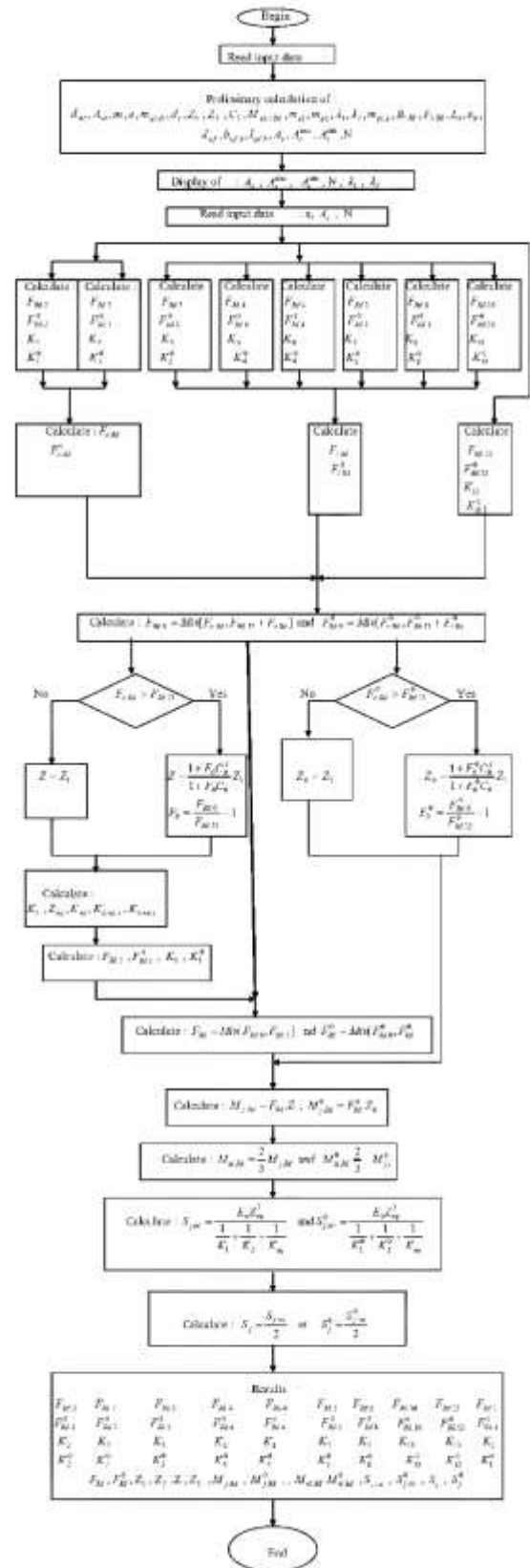


Figure 7. A- Flowchart of the RIMAX-1 computational algorithm for calculating the design moment resistance and initial rotational stiffness of composite beam-to-column joints with a non extended end plate based on the eurocode3/eurocode4 component method.

The program enables rapid evaluation of the joint design moment resistance ($M_{j,Rd}$) and initial rotational stiffness ($S_{j,ini}$), and facilitates systematic parametric studies for practical design assessment. Accordingly, the scope of the paper is limited to Eurocode-consistent analytical calculation and parametric interpretation, rather than independent experimental verification or full nonlinear joint modelling.

3. Results and Discussions

3.1 The influence of the longitudinal reinforcement ratio (μ) of the concrete slab

To evaluate the contribution of composite action to the global joint behavior, a parametric analysis was conducted varying the longitudinal reinforcement ratio (μ) of the concrete slab from 0.45% to 0.621%. The study evaluated a concrete-encased HEB 140 column and an IPE 220 beam, comparing the performance of a limited end-plate configuration against a non-extended end-plate. The quantitative results for design resisting moment and initial rotational stiffness are graphically and tabularly represented in Figures 8 and 9, respectively.

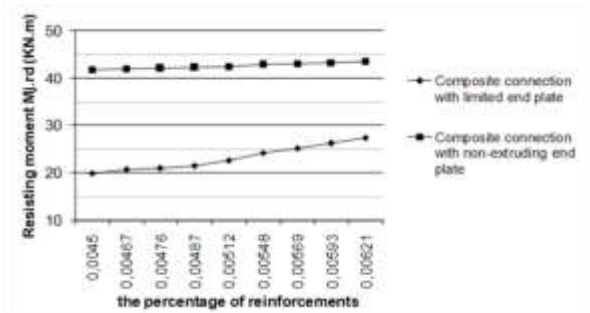


Figure 8. Variation of the resisting moment as a function of the percentage of the longitudinal reinforcements of the concrete slab (for $F_{sk}=400 \text{ N/mm}^2$, a concrete encased column in HEB 140 and IPE 220 beam).

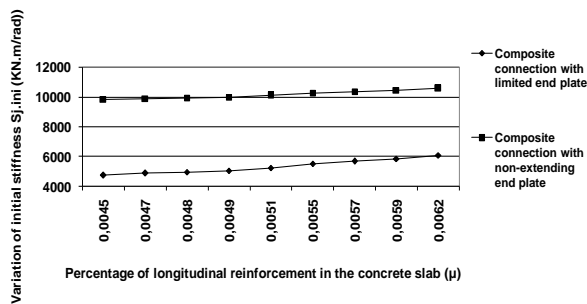


Figure 9. Variation of the initial stiffness $S_{j,ini}$ as a function of the percentage of the longitudinal reinforcements of the concrete slab (for $F_{sk}=400 \text{ N/mm}^2$, a concrete encased column in HEB 140 and IPE 220 beam).

Effect on Resisting Moment ($M_{j,Rd}$)

As shown in Figure 8, the sensitivity of the joint's moment capacity to the reinforcement ratio depends heavily on the end-plate topology. For the limited end-plate connection, the longitudinal reinforcement (Component 13) acts as the primary tensile load-bearing component. Consequently, increasing μ from 0.45% to 0.621% leads to a substantial increase of more than 27.53% in ($M_{j,Rd}$). Conversely, the non-extended end plate exhibits a much higher baseline capacity but is far less sensitive to reinforcement variations, showing only a 4.076% increase in ($M_{j,Rd}$) over the same range. This indicates a shift in the governing failure mechanism; in the non-extended configuration, the tensile resistance of the composite slab exceeds the capacity of the steel column's shear panel, meaning the column web (Component 1) becomes the limiting factor rather than the reinforcement.

Effect on Initial Stiffness

Figure 9 demonstrates a similar behavioral trend for joint rigidity. The participation of the end plate in the tension zone allows the non-extended configuration to be inherently stiffer. At the baseline reinforcement ratio ($\mu=0.45\%$), the non-extended end plate provides a massive 109.78% increase in baseline capacity and is 122.41% more rigid than the equivalent limited end-plate joint.

These findings underscore the importance of geometric topology in composite joint design. If an engineer opts for a limited end-plate connection, maximizing the slab reinforcement ratio is a highly effective method to boost both capacity and stiffness. However, if a non-extended end-plate is utilized, the steel components provide such substantial rigidity that over-reinforcing the concrete slab offers rapidly diminishing returns, allowing for potential cost savings in rebar detailing.

3.2 The influence of the beam profile height (H_b)

The geometric depth of the steel beam dictates the internal lever arm (Z) between the tension and compression zones, making it a fundamentally dominant parameter in joint mechanics. To quantify this effect, a parametric study was conducted varying the beam profile from IPE 160 to IPE 400 (H_b ranging from 160 mm to 400 mm) for a joint utilizing a concrete-encased HEB 400 column. The comparative results for moment capacity and initial stiffness are presented in Figures 10 and 11, respectively.

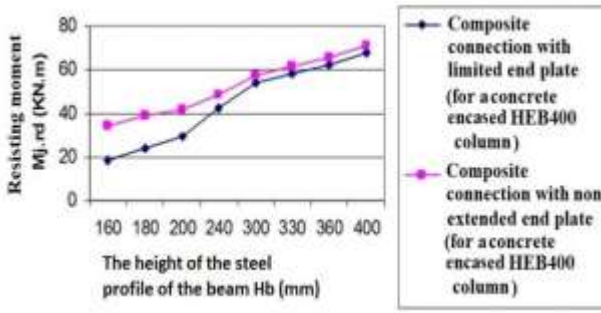


Figure 10. Variation of resisting moment as a function of the height of the steel profile of the beam.

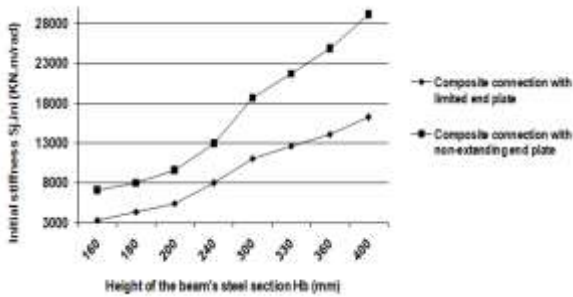


Figure 11. Variation of $S_{j,ini}$ as a function of the height of the steel profile of the beam.

Effect on Resisting Moment ($M_{j,Rd}$)

As illustrated in Figure 10, increasing the beam height leads to a significant increase in the moment resisting for both joint typologies. The participation of the end plate in the joints with a non-extended end plate significantly increases the resisting moment of the connection compared to the mixed connection with a limited end plate, reaching up to 83.068% (for an IPE 160 beam). This increase decreases gradually with increasing height of the steel profile of the beam until it reaches 5.735%, indicating that the two curves increasingly converge as H_b increases. Therefore, for large steel profiles of the beam in the mixed assembly, it is preferable to opt for a mixed connection with a limited end plate, as it provides resisting moment values ($M_{j,Rd}$) close to those of a mixed connection with a non-extended end plate (from the economic point of view and from the point of view of ease of implementation).

Effect on Initial Stiffness ($S_{j,ini}$)

Figure 11 demonstrates that while the two configurations converge in ultimate resisting moment, their elastic rigidity behaviors remain distinctly separated. The non-extended end plate completely dominates the stiffness profile because the flush plate extension provides continuous kinematic restraint against the column flange. At $H_b = 160$ mm, the non-extended plate is 110.944% stiffer than the limited end plate.

3.3 The influence of the end-plate thickness (t_p) for the non-extended configuration

To isolate the mechanical contribution of the end plate itself, a parametric sensitivity analysis was conducted on an HEB 180 column and IPE 220 beam assembly, varying the end-plate thickness (t_p) from 8 mm to 36 mm. The effects on design resisting moment ($M_{j,Rd}$) and initial stiffness ($S_{j,ini}$) are presented in Figures 12 and 13, evaluating both concrete-encased and non-encased column conditions.

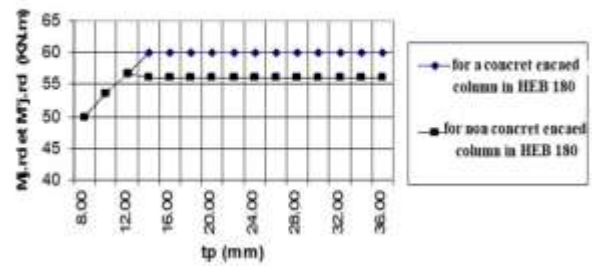


Figure 12. Variation of $M_{j,Rd}$ and $M^{\circ}j,Rd$ as a function of the thickness of the non-extended end plate

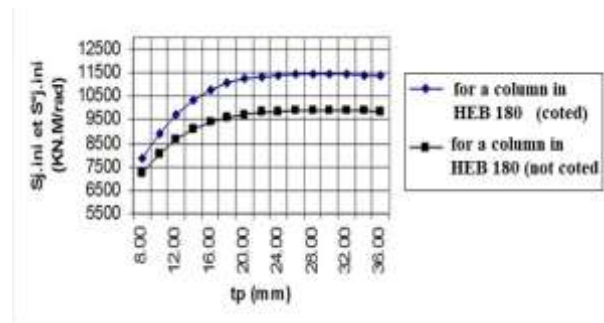


Figure 13. Variation of $S_{j,ini}$ and $S^{\circ}j,ini$ as a function of the thickness of the non-extended end plate

Effect on Resisting Moment ($M_{j,Rd}$)

Figure 12 demonstrates a strict, parameter-dependent threshold for ultimate joint capacity. For both column conditions, as the end-plate thickness increases from 8 mm to 12 mm, the resisting moment experiences an identical increase from 50.00 kN.m to 56.91 kN.m. However, beyond this point, a behavioral divergence occurs due to differing failure mechanisms. For the non-encased column, the capacity continues to grow until $t_p = 14$ mm, yielding a total 20.1% increase before plateauing at approximately 60.07 kN.m. This precise saturation point corresponds identically to the flange thickness of the HEB 180 column ($t_{fc} = 14$ mm). Once $t_p \geq t_{fc}$, no influence is recorded on the resisting moment. For the concrete-encased column, the moment capacity plateaus slightly earlier, stabilizing at approximately 56.31 kN.m (a 12.6% increase from

the baseline). This indicates that the introduction of concrete in the compression zone alters the internal stress distribution, activating a composite-specific limiting component (such as concrete crushing limits governed by Eurocode 4) before the steel plate can fully yield.

Effect on Initial Stiffness ($S_{j.ini}$)

Conversely, Figure 13 reveals that joint rigidity does not saturate simultaneously with moment capacity. While resistance maximizes around 14 mm, the initial stiffness continues to grow logarithmically until approximately 24-30 mm. before flattening. For the concrete-encased column, increasing t_p from 8 mm to 30 mm yields a massive 43.2% increase in stiffness (from 7,701.5 to 11,030.0 kN.m/rad). For the non-encased column, the stiffness increases by 34.4% (from 7,165.0 to 9,633.4 kN.m/rad). Furthermore, the data confirms that at the optimal geometric plateau, concrete encasement consistently provides a 14.5% baseline rigidity advantage over bare steel columns.

3.4 The effect of the presence of the second row of tension bolts

The results of the resisting moment and the initial Stiffness obtained by the calculation of the Composite joints a single row and for two rows of bolts in tension using the calculation software aim to see the double effect of the thickness of the plate and the presence of a second row of bolts in tension on the resisting moment and the initial rigidity The effect of the number of bolt rows in tension is shown in Figures 13 to 15. For the concrete-encased HEB180-IPE220 joint, increasing the number of tension bolt rows from one to two increased the design moment resistance from 50.02 to 52.21 kN·m at $t_p = 8$ mm and from 60.12 to 62.93 kN·m at $t_p = 30$ mm. The gain therefore ranges from about 4.4% to 4.7%, indicating a consistent but moderate

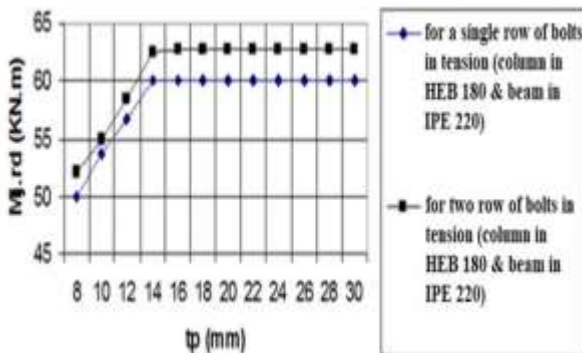


Figure 14. Variation of $M_{j.rd}$ as a function of the thickness of the non-extended end plate and the number of rows of bolts in tension (concrete encased column)

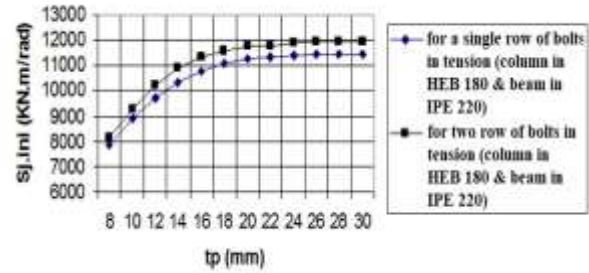


Figure 15. Variation of $S_{j.ini}$ as a function of the thickness of the non-extended end plate and the number of rows of bolts in tension (concrete encased column)

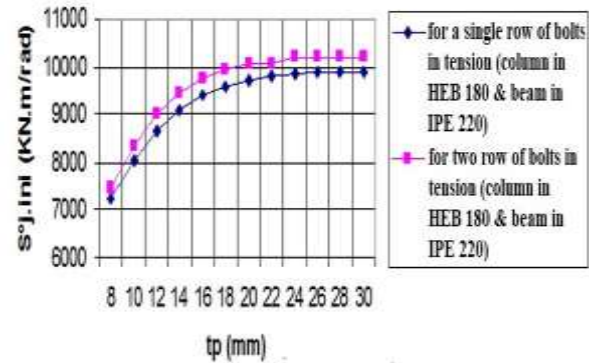


Figure 16. Variation of $S_{j.rd}$ as a function of the thickness of the non-extended end plate and the number of rows of bolts in tension (non-concrete encased column)

improvement in moment resistance. The influence on initial stiffness is more pronounced. For the concrete-encased column, the initial stiffness increased from 7875.09 to 8208.21 kN·m/rad at $t_p = 8$ mm and from 11479.40 to 11987.62 kN·m/rad at $t_p = 30$ mm. For the non-encased column, the corresponding increase was from 7266.02 to 7500.92 kN·m/rad at $t_p = 8$ mm and from 9904.82 to 10270.90 kN·m/rad at $t_p = 30$ mm. These results show that adding a second bolt row improves both resistance and stiffness, but the gain remains limited once the plate thickness becomes sufficiently large. This again confirms that the overall joint response is governed by the interaction among components rather than by a single detail. The second bolt row improves the tensile load distribution and stiffens the tension side of the joint.

To synthesize the complex mechanical behaviors observed in this study, Table 5 provides a comprehensive quantitative summary of the parametric sensitivity analysis. This table highlights the isolated influence of each investigated parameter on the joint's design resistance ($M_{j.Rd}$) and initial stiffness ($S_{j.ini}$), alongside the dominant interaction effects and structural thresholds identified by the RIMAX-1 analytical software.

Table 5. Quantitative summary of parametric sensitivities for the composite beam-to-column joint

Evaluated Parameter	Studied Range	Joint configuration	Effect on $M_{j,Rd}$	Effect on $S_{j,ini}$
Slab Reinforcement Ratio (μ)	0.45% to 0.621%	Non-extended end plate	Low sensitivity (4.07% increase)	High baseline stiffness (122.41% stiffer than limited)
		Limited end plate	Highly sensitive (27.53% increase)	Marked stiffness increase with reinforcement; response is highly sensitive to μ
Beam Profile Height (H_b)	160 mm to 400 mm. (IPE 160 to IPE 400)	Non-extended end plate	High increase (up to 83.06% at IPE 160)	Stiffness remains clearly higher than limited end plate; advantage reaches +110.94% at $H_b = 160$ mm
		Limited end plate	$M_{j,Rd}$ increases strongly with H_b , approaching the non-extended end-plate values at large beam sizes	$S_{j,ini}$ increases with H_b , but remains consistently lower than the non-extended end plate
End-Plate Thickness (t_p)	8 mm to 36 mm	Non-extended end plate	Saturates at $t_p = 14$ mm (max 20.1% increase)	Logarithmic growth, saturates between 24-30 mm
		Limited end plate	Variable	Variable
Tension Bolt Rows	1 Row vs. 2 Rows	Non-extended end plate	Moderate gain (4.4% to 4.7%)	Noticeable gain (up to 7.9% increase)
		Limited end plate	Moderate gain	Moderate gain
Concrete Encasement	Steel Profile Column vs. Concrete-Encased Column	Non-extended end plate	Saturates earlier (12.6% vs 20.1% gain)	14.5% baseline rigidity advantage
		Limited end plate	Modest capacity gain	Improved stiffness

3.5. Discussion and Theoretical Implications

The parametric findings extracted via the RIMAX-1 software strongly align with recent literature on composite joint behavior, while offering new quantitative thresholds. The observed saturation effect of the end-plate thickness—where moment capacity ceases to increase once the plate thickness surpasses the column flange thickness (t_{fc}) conceptually corroborates the finite element observations by [16], [22]. Their studies indicated that oversized end-plates merely shift the failure mode to the column without adding global capacity. Our Delphi-based analytical tool successfully and instantly quantifies this exact threshold for composite configurations without the need for computationally heavy 3D modeling. Furthermore, the varying sensitivity to the longitudinal reinforcement ratio (μ) addresses phenomena reported by [20]. While previous authors noted that increasing reinforcement generally improves capacity, our software's rapid comparative analysis clarifies that this is heavily dictated by the end-plate topology. In non-extended end plates, the high rigidity of the steel components causes the column web panel to govern prematurely, rendering excessive slab reinforcement redundant.

4. Conclusions

This study applied the Eurocode [1], [2] component method to composite beam-to-column joints with a

non-extended end plate and implemented the codified analytical procedure in a dedicated computational program developed in Delphi using object-oriented programming for evaluating the two principal design-oriented mechanical characteristics of the joint, namely the design moment resistance $M_{j,Rd}$ and the initial rotational stiffness $S_{j,ini}$.

The parametric investigation showed that the influence of slab longitudinal reinforcement depends strongly on the connection configuration: in the limited end-plate joint, increasing the reinforcement ratio from 0.45% to 0.621% increased $M_{j,Rd}$ by up to 27.53%, whereas the corresponding increase was much smaller in the non-extended end-plate joint because the governing mechanism shifted from slab reinforcement to steel joint components. Beam section height was identified as one of the dominant parameters controlling resistance, with the increase from IPE 160 to IPE 400 producing gains in $M_{j,Rd}$ of up to 83.07%, while the non-extended end-plate configuration maintained a substantial stiffness advantage over the limited end-plate configuration, reaching 110.94% in the studied range. The results also showed that end-plate thickness has a threshold effect: once the plate thickness approaches the connected flange thickness, further increases produce negligible improvement in resistance and only limited additional stiffness, indicating that over-dimensioning of the plate is not structurally efficient. The addition of a second row of tension bolts and the use of concrete encasement improved

the initial rotational stiffness, although their effect on resistance remained comparatively moderate. These findings confirm that joint behavior is governed by the interaction between slab participation, member geometry, and local connection detailing, and that the most effective design strategy depends on whether the target is strength enhancement or stiffness enhancement. The principal contribution of the study is therefore not the development of a new mechanical model, but the implementation of the Eurocode component method in a fast and useful computational framework that enables routine calculation and systematic parametric assessment of composite joint characteristics. From a practical perspective, the developed tool can assist engineers in selecting efficient joint details and in avoiding unnecessary material increase without proportional mechanical benefit.

Author Statements:

- **Ethical approval:** The conducted research is not related to either human or animal use.
- **Conflict of interest:** The authors declare that they have no known competing financial interests or personal relationships that could have appeared to influence the work reported in this paper
- **Acknowledgement:** The authors declare that they have nobody or no-company to acknowledge.
- **Author contributions:** The authors declare that they have equal right on this paper.
- **Funding information:** The authors declare that there is no funding to be acknowledged.
- **Data availability statement:** The data that support the findings of this study are available on request from the corresponding author. The data are not publicly available due to privacy or ethical restrictions.

References

- [1] B. EN, “1-1: 2004 Eurocode 4-Design of composite steel and concrete structures-Part 1-1: General rules and rules for buildings,” *Br. Stand. Inst. Lond. UK*, 1994.
- [2] C. EN, “1-1, Eurocode 3: Design of steel structures,” *Gen. Rules Rules Build.*, 1993.
- [3] A. Braconi, W. Salvatore, R. Tremblay, and O. S. Bursi, “Behaviour and modelling of partial-strength beam-to-column composite joints for seismic applications,” *Earthq. Eng. Struct. Dyn.*, vol. 36, no. 1, pp. 142–161, 2007, doi: 10.1002/eqe.629.
- [4] C. Amadio, C. Bedon, and M. Fasan, “Numerical assessment of slab-interaction effects on the behaviour of steel-concrete composite joints,” *J. Constr. Steel Res.*, vol. 139, pp. 397–410, Dec. 2017, doi: 10.1016/j.jcsr.2017.10.003.
- [5] Y. Xiao, L. Zeng, Z. Cui, S. Jin, and Y. Chen, “Experimental and analytical performance evaluation of steel beam to concrete-encased composite column with unsymmetrical steel section joints,” *Steel Compos. Struct.*, vol. 23, no. 1, Art. no. 1, Jan. 2017.
- [6] L. Chu, Q. Li, J. Zhao, and D. Li, “Seismic behavior of hybrid frame joints between composite columns and steel beams,” *Shock Vib.*, vol. 2020, no. 1, p. 8870582, 2020.
- [7] R. Senthilkumar and S. R. Satish Kumar, “Seismic performance of semi-rigid steel-concrete composite frames,” *Structures*, vol. 24, pp. 526–541, Apr. 2020, doi: 10.1016/j.istruc.2020.01.046.
- [8] Rafaela, G. Balaskas, C. Vulcu, and B. Hoffmeister, “Steel and composite joints with dissipative connections for MRFs in moderate seismicity – Experimental and numerical programs,” *Steel Constr.*, vol. 16, no. 1, pp. 31–43, 2023, doi: 10.1002/stco.202200044.
- [9] S. Park, P. Clayton, M. D. Engelhardt, T. A. Helwig, and E. B. Williamson, “Cyclic Response of Composite Steel Gravity Framing Connections in Multibay System-Level Tests | Journal of Structural Engineering | Vol 150, No 3,” Mar. 2023, Accessed: Mar. 22, 2026. [Online]. Available: <https://ascelibrary.org/doi/10.1061/JSENDH.STEN G-12998>
- [10] R. Don, G. Balaskas, C. Vulcu, and B. Hoffmeister, “Full-Scale Composite Moment-Resisting Frame with Dissipative Bolted Connections under Monotonic Loads: Experimental versus Numerical Results,” *ce/papers*, vol. 6, no. 3–4, pp. 1356–1361, 2023, doi: 10.1002/cepa.2250.
- [11] K. Chen and B. Yang, “Component-based modeling for steel and composite beam-column joints subjected to quasi-static and impact loads under column removal scenarios,” *J. Struct. Eng.*, vol. 149, no. 11, p. 04023149, 2023.
- [12] K. Ma *et al.*, “Seismic behavior and initial rotational stiffness of beam-to-column composite connection in steel frame,” *Structures*, vol. 62, p. 106069, Apr. 2024, doi: 10.1016/j.istruc.2024.106069.
- [13] M. Fasan, C. Bedon, C. Amadio, and M. R. Pecce, “Non-linear component-based modelling strategy for beam-to-column steel-concrete composite joints under seismic loads,” *J. Constr. Steel Res.*, vol. 212, p. 108314, 2024.
- [14] A. Ajwad, S. Di Benedetto, M. Latour, and G. Rizzano, “A component method approach for single-sided beam-to-column joints with CHS column and welded double-tee beam,” *Thin-Walled Struct.*, vol. 202, p. 112055, 2024.
- [15] M. B. Bozkurt and M. D. Engelhardt, “Effect of Composite Gravity Framing on Seismic Response of Eccentrically Braced Frames,” *Turk. J. Civ. Eng.*, no. Advanced Online Publication, 2025, Accessed: Mar. 22, 2026. [Online]. Available: <https://dergipark.org.tr/en/pub/tjce/article/1726766>

- [16] X.-Z. Feng, X.-C. Liu, X. Chen, W. Zhou, and K. Meng, "Seismic performance of joints for a novel composite beam and cruciform thin concrete encased steel column," *J. Constr. Steel Res.*, vol. 239, p. 110234, Apr. 2026, doi: 10.1016/j.jcsr.2026.110234.
- [17] P. Bourrier and J. Brozzetti, "Construction métallique et mixte acier-béton, calcul et dimensionnement selon EC3 et EC4," *APK Édition Eyrolles Paris*, 1996.
- [18] L. F. L. Ribeiro, R. M. Gonçalves, and C. A. Castiglioni, "Beam-to-column end plate connections—An experimental analysis," *J. Constr. Steel Res.*, vol. 46, no. 1–3, pp. 264–266, 1998.
- [19] L. Simões da Silva, R. D. Simões, and P. J. S. Cruz, "Experimental behaviour of end-plate beam-to-column composite joints under monotonical loading," *Eng. Struct.*, vol. 23, no. 11, pp. 1383–1409, Nov. 2001, doi: 10.1016/S0141-0296(01)00054-2.
- [20] A. Ataei, H. Keighobadi, A. A. Chiniforush, and T. D. Ngo, "Experimental study of exterior beam-to-column composite joint with precast concrete slab and demountable embedded bolted shear connector," *J. Build. Eng.*, vol. 117, p. 114821, Jan. 2026, doi: 10.1016/j.job.2025.114821.
- [21] A. Abidelah, "Analyse numérique du comportement d'assemblages métalliques. Approche numérique et validation expérimentale," These de doctorat, Clermont-Ferrand 2, 2009. Accessed: Jun. 11, 2025. [Online]. Available: <https://theses.fr/2009CLF21965>
- [22] S. B. Merad Boudia, N. Boumechra, A. Bouchair, and A. Missoum, "Modeling of bolted endplate beam-to-column joints with various stiffeners," *J. Constr. Steel Res.*, vol. 167, p. 105963, Apr. 2020, doi: 10.1016/j.jcsr.2020.105963.
- [23] T. Tougui, H. Darnif, E. Azelmad, Z. Maskaoui, and L. Bousshine, "Finite Element Analysis of a Semi-Rigid Endplate Beam-to-Column Joint with Stiffeners," 2023.
- [24] J.-F. Demonceau and A. Ciutina, "Characterisation of beam-to-column steel-concrete composite joints beyond current Eurocode provisions," presented at the Structures, Elsevier, 2019, pp. 167–175.
- [25] J.-F. Demonceau, "Design of beam-to-column steel-concrete composite joints: From Eurocodes and beyond," in *Modern Trends in Research on Steel, Aluminium and Composite Structures*, Routledge, 2021, pp. 14–24.
- [26] S. Chen, K. Chen, and K. H. Tan, "Effect of profiled decking on composite beam-column joints with end-plate bolted connections under column-removal scenario," *J. Constr. Steel Res.*, vol. 182, p. 106668, Jul. 2021, doi: 10.1016/j.jcsr.2021.106668.
- [27] M. A. Bennacer, A. Beroual, A. Kriker, and J.-F. Demonceau, "Analytical model for composite joints under sagging moment," *Eng. Struct.*, vol. 101, pp. 399–411, Oct. 2015, doi: 10.1016/j.engstruct.2015.07.024.
- [28] R. S. Nicoletti, A. S. de Carvalho, A. S. C. de Souza, and S. J. de Castro Almeida, "Evaluation of the Behavior of Composite Double Web-Angle Connections at Ambient Temperature and in a Fire Situation: Evaluation of the Behavior of Composite Double Web-Angle," *Fire Technol.*, vol. 61, no. 4, pp. 1809–1860, 2025.
- [29] A. Abdulkarim, A. Ataei, and H. T. Riahi, "Experimental Evaluation of Deconstructable External Composite Joints with Stiffened End-Plates and Bolted Shear Connectors under Cyclic Loading," *J. Build. Eng.*, p. 115545, 2026.
- [30] A. Abidelah, A. Bouchair, and D. E. Kerdal, "Experimental and analytical behavior of bolted end-plate connections with or without stiffeners," *J. Constr. Steel Res.*, vol. 76, pp. 13–27, Sep. 2012, doi: 10.1016/j.jcsr.2012.04.004.
- [31] F. M. Shaker and W. M. Abd Elrahman, "Behavior of flush and extended end-plate beam-to-column joints under bending and axial force," *World Appl. Sci. J.*, vol. 30, no. 6, pp. 685–695, 2014.
- [32] M. A. Bennacer, H. Necib, S. Amara, A. Beroual, and O. Brai, "New design model for the slab reinforcement in external steel-concrete composite joints under sagging moment," *Stud. Eng. EXACT Sci.*, vol. 5, no. 2, p. e11820, Dec. 2024, doi: 10.54021/seesv5n2-687.
- [33] H.-J. Lee and H.-G. Park, "Seismic behavior of precast concrete beam-column joints with encased steel tube," *J. Build. Eng.*, vol. 61, p. 105296, Dec. 2022, doi: 10.1016/j.job.2022.105296.
- [34] Y. Tao, S. Feng, Y. Yang, J. Ye, and W. Zhao, "Experimental study on seismic behavior of RC column-steel beam joints with whole column-section diaphragm," *Eng. Struct.*, vol. 299, p. 117100, Jan. 2024, doi: 10.1016/j.engstruct.2023.117100.
- [35] J. Duan, D. Yang, X. Liu, and P. Xiang, "Seismic Energy Dissipation and Hysteresis Performances of Distinctly Shaped Steel-Reinforced Concrete Column-Beam Joints under Cyclic Loading," *Buildings*, vol. 14, no. 9, Art. no. 9, Sep. 2024, doi: 10.3390/buildings14092777.
- [36] V.-P. Nguyen, Q.-H. Nguyen, M. Couchaux, J. M. Aribert, and M. Hjiat, "Hybrid steel beam to exterior RC column joints with encased steel profile," *Eng. Struct.*, vol. 306, p. 117624, May 2024, doi: 10.1016/j.engstruct.2024.117624.
- [37] J. Zeng, W. Lu, and J. Paavola, "Analytical models for predicting the load-bearing strength of beam-to-column joints in a composite steel frame," *Thin-Walled Struct.*, vol. 157, p. 107100, Dec. 2020, doi: 10.1016/j.tws.2020.107100.
- [38] H.-J. Lee, H.-G. Park, I.-R. Choi, and H.-J. Hwang, "Tensile and flexural behaviors of connections between steel beam and concrete-encased-and-filled steel tube column," *J. Build. Eng.*, vol. 49, p. 104042, May 2022, doi: 10.1016/j.job.2022.104042.
- [39] Y. Zhu, W. Wang, Y. Shi, L. Bao, M. Li, and S. Wang, "Finite element modeling and design equations of partially steel-reinforced concrete beam-to-steel tube column joint," *Structures*, vol. 57, p. 105172, Nov. 2023, doi: 10.1016/j.istruc.2023.105172.

- [40] Y. Zhu *et al.*, “Experimental and numerical study on seismic behavior of partially steel-reinforced concrete beam-to-steel tube column joint,” *J. Build. Eng.*, vol. 76, p. 107210, Oct. 2023, doi: 10.1016/j.jobbe.2023.107210.